Chapter 14
Crack Detection and Localization in Thermoelectric Wafers using Vibroacoustic Excitation

Thomas C. Magee, Angel F. Bravo, Sterling B. Rawls, John J. Greenhall, Nicholas A. J. Lieven, Milo G. Prisbrey, and Neel Shah

Abstract Thermoelectric materials convert electrical energy to thermal energy and vice versa via the Peltier and Seebeck effects. These thermoelectric wafers have applications such as radioisotope thermoelectric generators (RTGs) in spacecraft and solid state refrigeration systems. However, thermoelectric wafers are brittle and thus susceptible to microscopic cracking during manufacturing, which compromises the thermoelectric conversion efficiency and the structural integrity of the material in service. Cracks in the wafers are traditionally detected and localized via manual human-inspection (i.e. via microscopy), which is time intensive and prone to human error. Alternatively, acoustic resonance can be employed to detect cracks, which affect the natural resonance modes of the wafer. In these techniques, crack detection involves measuring the vibration amplitude at a single location on the wafer surface across a range of ultrasonic excitation frequencies. High vibration amplitudes corresponding with resonance modes that are dependent on each sample's geometry, and thus change if cracks are present. In this work, we extend the capabilities of previous acoustic resonance techniques to include crack localization capabilities while reducing scan times by identifying and measuring the mode shape for a small number of resonance frequencies. When a crack is present near an antinode of a resonance mode, where the vibration amplitude is maximum, a sharp discontinuity is present in the measured mode. We present a method to automate the crack detection and localization process using image processing methods to detect the discontinuities within the measured modes. We demonstrate the technique experimentally on thermoelectric wafers (N=31), for which we achieve a detection accuracy of 90.3% and localization error of 2.2%. Additionally, the new technique enabled measuring crack length with 17.8% error, compared to manually inspected microscope scans.

Keywords thermoelectric · vibroacoustic · crack · detection · localization · frequency response

Introduction

Thermoelectric materials (TEMs) have wide ranging applications in solid-state electronics. Thermoelectric compounds, such as Bismuth Telluride (Bi_2Te_3), are capable of the interconversion of electrical and thermal energy via the Peltier and Seebeck

Thomas C. Magee
Department of Physics & Astronomy, Department of Aerospace Engineering, Texas A&M University, College Station, TX 77843
e-mail: tmagee@lanl.gov

Angel F. Bravo
Department of Mechanical and Aerospace Engineering, The University of Texas at El Paso, El Paso, TX 79968
e-mail: afbravo@lanl.gov

Sterling B. Rawls
Department of Structural Engineering, University of California San Diego, La Jolla, CA 92093
e-mail: srawls@lanl.gov

John J. Greenhall · Milo G. Prisbrey · Neel Shah
Los Alamos National Laboratory, Los Alamos, NM 87545
e-mail: jgreenhall@lanl.gov; mprisbrey@lanl.gov

Nicholas A. J. Lieven
University of Bristol, Bristol BS8 1TH, UK
e-mail: Nick.Lieven@bristol.ac.uk

Brandon Dilworth et al. (eds.), *Topics in Modal Analysis & Parameter Identification I, Vol. 9*, Conference Proceedings of the Society for Experimental Mechanics Series, https://doi.org/10.13052/97887-438-0154-2_14

effects [1]. As a result, thermoelectric wafers are found in numerous applications ranging from microprocessor coolers and medical devices to solid-state refrigeration systems and radioisotope thermoelectric generators (RTGs) in spacecraft [1], [2].

TEMs such as the Bi_2Te_3 samples discussed in this paper are initially manufactured as thin wafers (roughly 0.5mm thick) that are sectioned into smaller constituents to match the scale and operational parameters of different thermoelectric modules. Due to the manufacturing process and intrinsic characteristics of TEMs (especially Bi_2Te_3), the wafers are brittle and are susceptible to cracking. The presence of cracks in TEMs greatly reduces the efficiency of the electrical-thermal interconversion by preventing optimal current and thermal flux across the wafer [1]. However, processing cracked TEMs to the point at which the current and thermal flux can be measured would result in substantial losses in terms of cost and production time. Thus, it is paramount that cracks are detected in TEMs early in the production process so the wafer can be discarded or undamaged sections can be salvaged.

Current state-of-the-art methods for detecting cracks in the wafers include inspection via optical microscopy [3], X-ray micro computed tomography (micro-CT) [4], and single point ultrasound assessment [5], [6]. In optical microscopy examination, each wafer is examined manually in the search of cracks and surface defects. However, it is time intensive and subject to errors due to various lighting conditions and surface defects or variance in operator skill. While advancements have been made in the automation of microscopic examination and analysis [7], the process is still limited in application to thermoelectric wafers due to the aforementioned reasons. X-ray micro-CT is capable of detecting cracks where density of air within the crack is much lower than that of the wafer. It, however, has limited scanning resolution of 50-100 μm, which can result in cracks smaller than this limit being missed. It also requires excessive scanning time (often $>$24 hrs) and expensive equipment [4]. Alternatively, ultrasound has been used to detect microcracks based on changes in the measured frequency response [6], [8]. When cracks are excited, the wafers exhibit Contact Acoustic Nonlinearity (CAN) wherein the vibrations cause the cracks to periodically open and close, resulting in nonlinear artifacts in the measured frequency response.

Frequency response analysis of a single-point ultrasonic excitation can inform whether or not a crack is present in the wafer but cannot localize cracks. To localize the cracks, the vibrational modes must be measured by scanning over the surface of the wafer. This can be achieved by exciting the wafer over a range of frequencies via chirp burst or frequency-sweep. The frequency response across the wafer surface is measured one location at a time using a laser Doppler vibrometer (LDV), which uses either a mechanical stage to scan the wafer or mirrors to adjust the laser position. This results in a measurement of the frequency response across the entire wafer over a range of user-specified frequencies. Scanning times for this process are dependent on the resolution and range for both frequency and spatial dimensions, but tend to be on the order of 1-2 hrs for the measurement parameters necessary to detect cracks in TEM wafers. As a result, crack localization using traditional LDV methods is infeasible for the production rates needed in an industrial manufacturing setting. Greenhall et al. employed the ultrasonic frequency-sweep method with a mechanical stage to detect cracks in thermoelectric wafers [6]. Results from Greenhall's method, which will be referred to as the mechanical scan method for the remainder of this paper, were used to develop the foundations of the presented crack detection and localization technique.

To implement ultrasonic crack detection and localization with reasonable scanning times for production-scale quality control, we present a new scanning method, wherein we use an LDV to perform spatial sweeps over the sample excited at a small number of preselected resonant frequencies. This significantly reduces the amount of time that the LDV needs to measure each point on the wafer. In doing so we are able to scan over wafers in minutes instead of hours or days. Additionally, we have developed an algorithm employing image processing methods to detect and characterize any present cracks with respect to location and size. A more complete description of this scanning technique, along with the methods applied to determine the critical excitation frequencies for each sample and subsequent post processing, is further described in § 2. Results of this novel technique are presented in § 3 and concluding remarks are presented in § 4.

Methods

When a wafer is excited at a resonance frequency, the resonance mode, i.e. vibration pattern of the wafer, can be recorded by measuring the vibrations across the surface of the wafer with a scanning LDV. When a crack is present near an antinode, where the vibration amplitude is maximum, discontinuities are observed in the measured vibrational response at the crack location. This discontinuity can be exploited in image processing to detect and localize cracks. To determine the full length of a propagated crack this technique requires high vibration amplitude at all positions where cracks may be present. To detect cracks throughout the wafer, multiple resonant frequencies must be measured to obtain a variety of mode shapes, so that all areas of the wafer will contain an antinode for at least one resonance mode. This could be completed using previously mentioned ultrasonic methods, which excite a broad range of frequencies, but these incur long measurement times. Additionally, these methods measure responses between resonance frequencies, resulting in extreme datasets of mostly low response. Thus, we present a measurement method that only measures responses at select resonance frequencies, which drastically reduces the required measurement time. This technique builds off of Los Alamos National Lab's Acoustic Steady-State Excitation Spatial Spectroscopy (ASSESS) used for structural health monitoring and thickness estimations in a variety of materials and geometries [9].

This section will describe the setup and execution of the spatial scan process referred to as rapid resonance mode scanning. It will then explain how the chosen excitation frequencies of the wafer are determined via reduced-scan single point ultrasound assessment. With an understanding of how the new experimental data are obtained, this section will then describe the image processing techniques applied to the resonance mode scan data to isolate, detect, and locate any cracks present on each analyzed thermoelectric wafer.

Rapid resonance mode scanning

In rapid resonance mode scanning, a thermoelectric wafer is excited at a single resonance frequency and the LDV scans over a rectangular region extending past the wafer's edges as to measure a single resonance mode shape. For each wafer, we repeat this process at four resonance frequencies, resulting in four resonance mode shapes. An example collection of mode shapes at each frequency is shown in Fig. 2. Here, the four resonance frequencies are selected to ensure that all potential crack locations are sufficiently close to an antinode so that they will be excited by at least one resonance mode, while also keeping the number of excited resonance frequencies low to reduce the scan time (see § 2.2 for details).

From the four resonance mode shapes in Fig. 2, we observe discontinuities in the upper- and lower-left corners, which correspond to known crack locations. We also observe that each frequency used produces different mode shapes through the wafer that highlight cracking in different locations on the wafer. This qualitatively illustrates how ultrasound mode shape imaging enables crack detection and localization (see § 2.3 for details).

Selection of excitation frequencies

Before a wafer's resonance mode shapes are measured, the resonance frequencies are experimentally determined for each sample. The selection of various resonant frequencies ensure that the every location on wafer is sufficiently close to an antinode of at least one resonance mode to ensure detection of cracks anywhere on the wafer. To measure the resonance frequencies of the wafer, we average the frequency response measured over a range of frequencies at three locations along the wafer diagonal, as shown in Fig. 3. Here, we excite the frequency range from 6kHz to 40kHz, which was empirically selected because it was found to contain resonances with antinodes that were sufficiently distributed across the sample geometry.

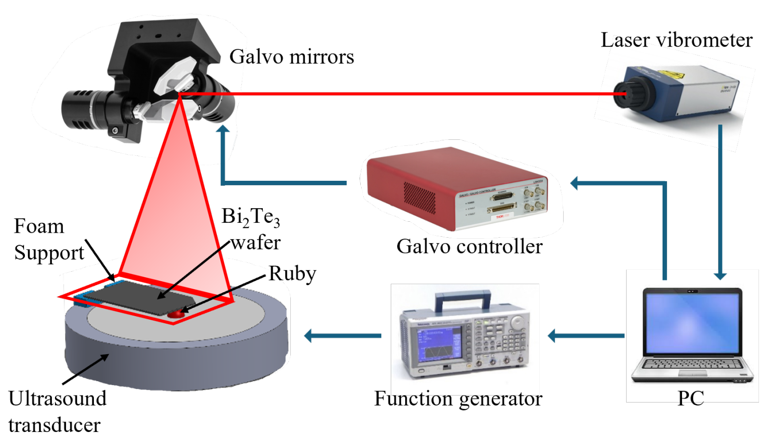

Fig. 1 Schematic of the experimental setup used in the rapid resonance mode scanning technique. A thermoelectric wafer (Bi_2Te_3) is placed in point-contact on an ultrasound transducer, balanced by foam supports. An LDV scans over the wafer surface using a set of galvo mirrors driven by a galvo controller. A function generator is used to excite the transducer at each resonance frequency, one at a time. A single computer controls the instruments and simultaneously records data obtained from the LDV.

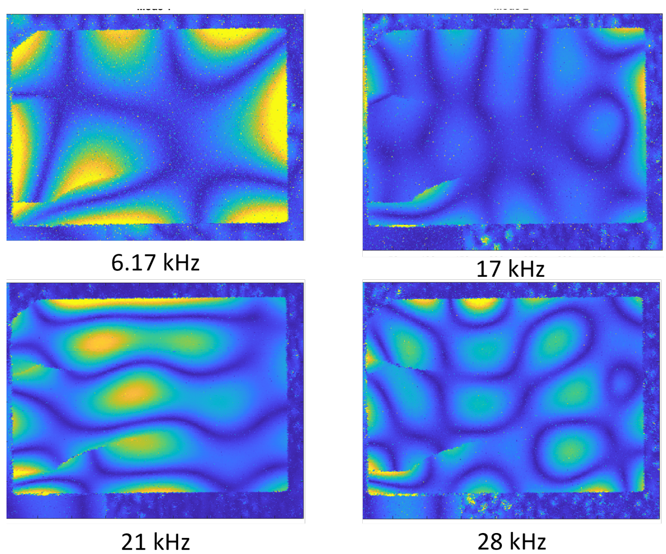

Fig. 2 Sample results of the rapid resonance mode scanning process. LDV scan outputs of a wafer scanned at four distinct resonant frequencies with modulated intensity to normalize the response amplitude. The varied mode shapes are selected to excite the full length of any possible defects in the wafer, which are present in the upper and lower left portions of the sample.

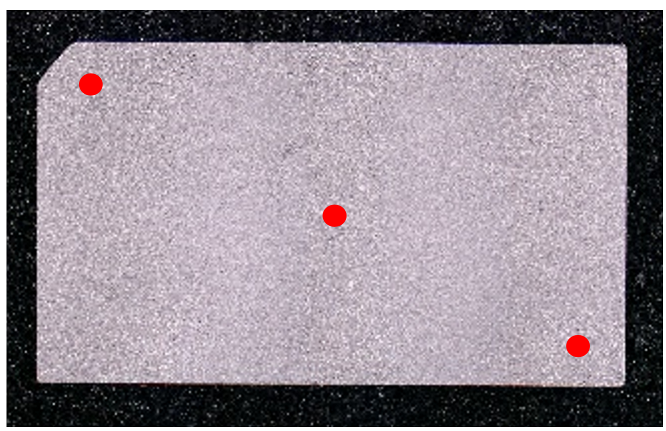

Fig. 3 Microscopic image of a sample with an overlay of 3 point locations along the diagonal. The three points along the diagonal are assessed using the LDV to obtain resonance peaks in an approximate frequency response.

The three measurement locations were selected to accurately measure the true resonance frequencies with a minimal number of measurement locations to reduce the overall measurement time. To determine the specific locations, the frequency spectrum was measured from 6 kHz to 40 kHz across the entire wafer surface for multiple wafers using chirp excitation and mechanical scanning. An example of this scan at a single frequency is shown in Fig. 4, where a cracked wafer is shown at a specific resonance frequency (28kHz). By averaging over all scan locations, we are able to obtain the frequency spectrum for the wafer, as shown in Fig. 5. Averaging is done here to ensure that all resonances are detected, even if they are missed by a measurement at a single location, i.e. if that location contains a resonance mode node. However, averaging over a scan of the entire wafer results in long data collection times (often $>$ 2 hours), which would reduce the applicability of the technique.

To obtain a sufficiently accurate approximation of the mean wafer behavior without scanning the entire wafer, we identify a small number of locations whose average frequency spectrum matches that of the overall wafer spectrum. Previously collected mechanical scans were analyzed to determine which points in the wafer geometry most accurately represent the mean wafer response across the full excitation spectrum. This was done by comparing the frequency response at each location to the total mean wafer response via Mean-Square Error (MSE). The total wafer response was calculated by spatially averaging each pixel's frequency response over the entire sample. The MSE process can be described as

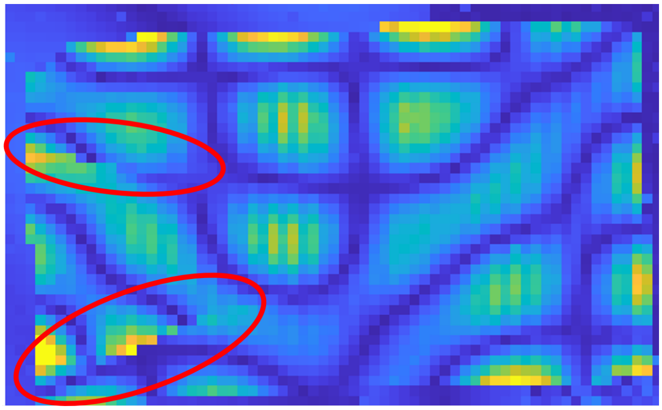

Fig. 4 Example of scan produced from the previous mechanical scanning technique on a cracked wafer at 28kHz. The assessment at the resonant frequency results in greater discontinuities at the edges of the wafer and regions of the cracks near anti-nodes. The presented scan was collected over a period of 2 hours.

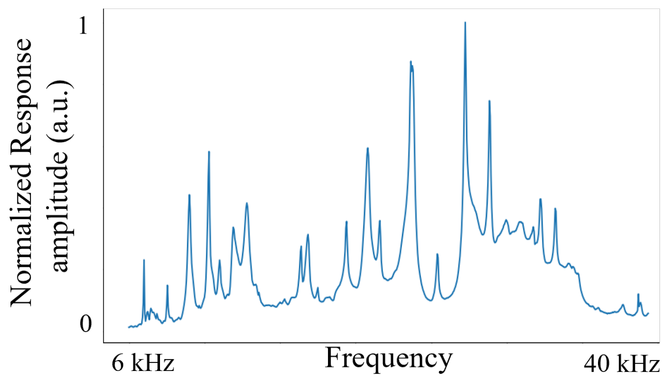

Fig. 5 Normalized frequency response of the full sample scan shown in Fig. 4. The normalization process performs a spatial average of the frequency response while incorporating scan data taken from the ultrasonic transducer below the wafer (on the outer bounds of the scan).

$$\tilde{a} = \frac{1}{N} \sum_{i=1}^{N} (a_i - \bar{a})^2, \tag{1}$$

where $\tilde{a}$ is the MSE, N is the total sample size, a_i is the frequency response at location i, and $\bar{a}$ is the spatially averaged frequency response of the analyzed sample. Equation 1 was applied to frequency responses of 13 previously analyzed wafers. From this analysis it was determined that points along the diagonal of the wafer geometry, presented in Fig. 3, most accurately represented the mean response.

Figure 6 shows an example mean response spectrum (blue) from the entire wafer compared to the combined response (red) from the three locations shown in Fig. 3. We observe that using three measurement locations results in dominant resonance frequencies that are equivalent to those of the entire wafer. From the approximated response using three measurement locations, excitation frequencies for the rapid resonance mode scans can be selected.

We use the mean frequency response to identify the resonance excitation frequencies used to measure the resonance mode shapes. We select resonance frequencies that will produce high vibration amplitudes throughout the wafer to ensure that cracks anywhere on the wafer will be detected. It is known that a response maximum is observed at a resonance frequency, but performing scans at resonance frequencies relatively close to each other (eg. peaks at 28kHz and 29.5kHz) have similar mode shapes and will therefore interrogate the same regions of the wafer. Selection criteria for the specific modes are based on spacing, prominence, and amplitude of the resonance peaks to ensure interrogation along the full length of any present defects.

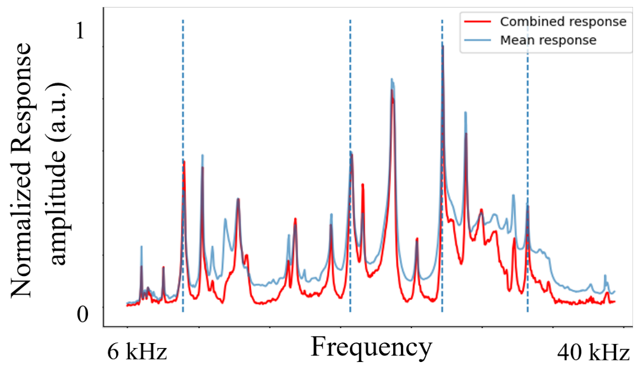

Fig. 6 Normalized frequency response of the full sample (blue) compared to the normalized approximate response from three points along the wafer's diagonal (red). In the approximate response, resonance peak behavior is conserved. Selected excitation frequencies for the rapid resonance mode scan (blue-dashed) are selected under spacing, prominence, and amplitude criteria.

The approximate mean response obtained from the three-point ultrasound assessment is used to select excitation frequencies for rapid resonance mode scanning. The selection of the assessment points used to create the approximate mean response is bolstered by MSE analysis of data collected using the mechanical scanning technique and is used to obtain wafer response characteristics in a fraction of the collection time previously required. The series of rapid resonance mode scans are performed at the selected excitation frequencies and image processing techniques are applied to detect, localize, and measure crack length and location on the resultant composite scan.

Image processing and crack localization

Following the spatial scanning process resulting in the scans presented in Fig. 2, each sample's scans undergo a series of image processing techniques to analyze the wafer and isolate any defects present on the sample. By searching for discontinuities in the samples response amplitude, the edges of the wafer and any cracks are qualitatively observed. An edge detection algorithm is applied to mask the edges of the wafer. This process isolates any defects present within the bounds of the wafer so that the discontinuities due to the edges of the wafer are not classified as cracks later on in the process. After masking the edges and detecting existing cracks on the wafer, the processed image then undergoes a series of quantification measures that automatically locate the centroid of the detected crack and calculate its length.

Prior to applying any form of image processing, a series of quality checks are performed on each of the four mode shape measurements to ensure that no detrimental artifacts are present that would reduce the accuracy of the processed scan. Quality checked scans then go through a series of edge and crack detection processes that enable the isolation, localization and quantification of any cracks.

Scan pre-processing

A common form of artifacting present in non-intrusive ultrasonic assessment with an LDV is classified as ”chatter”. Chatter can occur in both cracked and uncracked wafers when high excitation amplitudes from the ultrasonic transducer result in intermittent contact between the sample and transducer [6]. When present, chatter results in a high level of noise in the spatial scans and a distinct set of nonlinear response characteristics. When performing the spatial scans, the transducers excitation amplitude was tuned to maximize response amplitude without inducing chatter.

Another form of artifacting that occurred during this scan process was induced by scan speed limitations in the rapid-scan setup. If spatial scans were performed to quickly, horizontal artifacting would present on the resulting scan. The speed induced artifacting caused high response gradients that would be detected as cracks in the detection process and therefore limited the scan speed of the setup.

While there are other forms and causes of scan quality depreciation, those previously mentioned were most commonly addressed in the scanning process. Each recorded spatial scan was manually inspected for quality prior to being sent through the crack detection and localization process. The use of high quality scans in the crack detection process is necessary for accurate detection and localization of sample defects.

Edge detection and masking

Following the pre-processing quality check of the four scans preformed for each sample, an edge detection algorithm is applied to each scan. Based on mode shapes in the response, some of the images emphasize the edge of the wafer while others emphasize the crack present in the sample. This algorithm sums the four scans and returns a composite image with the combination of the modes where we can now see both the edges of the wafer and the cracks, as shown in Fig. 7.

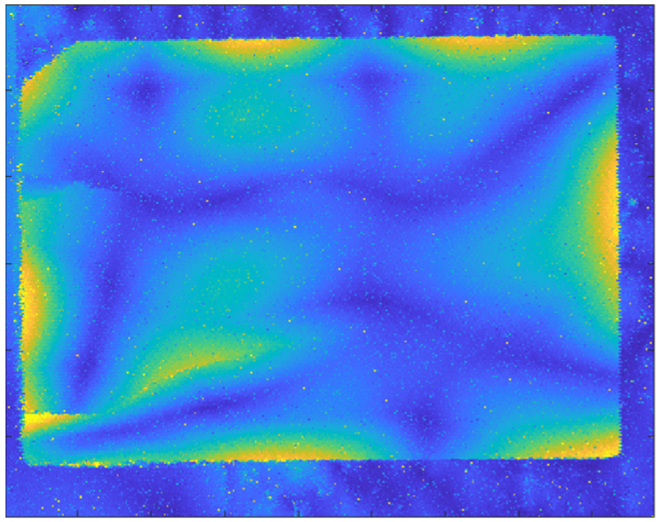

Fig. 7 Combined image of different modes extracted from the tests.

A bilateral filter is then applied to the composite image. The bilateral filter applies a Gaussian blurring to the image while preserving high gradient discontinuities [10]. Presented in Fig. 8, this process reduces any leftover artifacting while preserving the edges of the wafer and any present defects.

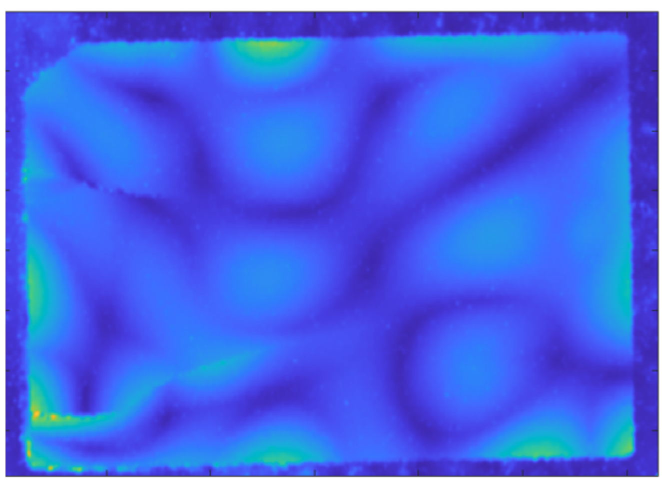

Fig. 8 Combined image with the bilateral filter applied.

A Canny edge detection function is then applied to the filtered image. The edge detection function serves to mark the edges of the wafer by returning a binary image of the high gradient regions of the input image [11]. Gaps were present in the edges of the sample after applying the Canny edge detection function at regions where the scan discontinuity at the edge was below the specified parameter. If the parameter was lowered past a critical value, mode shapes as those shown in Fig. 8 would be detected as edges. To accommodate the gaps left from the Canny edge detection, a convex hull was applied to the binary image.

Convex hull is an image processing technique that connects the outermost points in a binary image to enclose an area of interest [12]. In this specific application, the convex hull is applied to define the geometry bounded by the wafer's edges.

A perimeter detection algorithm is then applied to the binary image produced by the convex hull. This process isolates the outermost pixels of the wafer geometry leaving only the edges of the wafer. The result of the convex hull and perimeter isolation is presented in Fig. 9. This perimeter is then used to mask the edges of the wafer in the crack detection and quantification process.

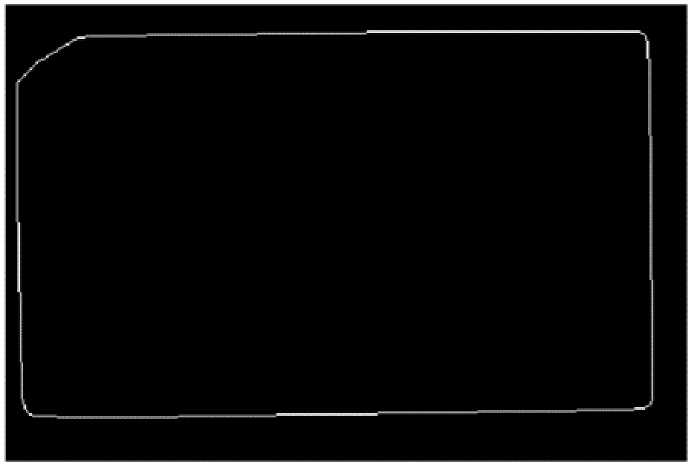

Fig. 9 Perimeter of the wafer obtained after applying convex hull and perimeter detection to the combined image after bilateral filtering is applied.

Crack detection and quantification

The edge detection and masking process serves to produce a bilateral image that enables the isolation of cracks present on the wafer sample. Before this image can be used, a series of processes need to be applied to the original spatial scans before the cracks can be isolated. The four spatial scans of the sample will each go through the bilateral filtering and Canny edge detection process to emphasize both the edges of the wafer and any present defects [10] [11]. For this process, each of the filtered images will go though the Canny edge detection with varied thresholds. The independent selection of thresholds for the four resonant scans enables the user to select the threshold that best shows the edges and defects on the wafer. Different thresholds will result in different produced crack lengths. Each resonance mode scan is put through the varied threshold edge detection process independently and the four resulting binary images are combined to a single composite that produces a full image of the cracks and edges. The result the composite binary image is shown in Fig. 10.

Fig. 10 Composite binary image of a wafer with cracks displaying both wafer edges and cracks present within the bounding geometry. This image is produced by applying Canny edge detection to each resonance mode scan independently and combining the resultant images.

The composite binary image produced from the four mode shape measurements will then have the edges of the wafer masked to isolate the cracks within the bounding geometry. The binary perimeter of the wafer shown in Fig. 9 is subtracted from the composite image of the full wafer. A morphological close function is applied the internal defects of the wafer remaining on the resulting binary image. The morphological close function serves to enclose the fine regions outlined by the bounds of detected cracks, essentially adding mass to their shape in the image [13]. The resulting binary image, depicted in Fig. 11, isolates the cracks and depicts the centroid locations of the detected defects.

With the internal defects of the wafer isolated and weighted in the binary image, the cracks can be quantified in both location and size with respect to the wafer geometry. The centroids are defined at the center of mass for each crack detected by the algorithm. coordinate locations of each centroid are recorded. Crack size is measured by calculating the distance between the end points of each detected crack.

Fig. 11 Binary image of the detected cracks on a sample after the edge masking and morphological filters are applied. The centroids of the detected cracks are calculated and shown as red stars.

By applying this series of image processing filters and techniques, cracks detected on scanned wafer samples are isolated and measured in both location and size. To verify the validity and accuracy of this technique, results are compared to a ground truth of manually assessed microscopic data.

Error quantification

To calculate the error of the algorithm, LDV scans of the new technique were compared to microscope scans for each wafer tested. The automatically detected cracks found in the LDV scans were compared in lenght andlocation to microscope scans that were manually mapped to find each crack and centroid coordinate location. By scaling the dimensions of the high resolution microscope scan to that of the LDV scanning technique, the centroid location determined by the image processing algorithm on the ultrasound can be compared to the centroid location of the scaled microscope scan. Centroid localization error is calculated as the distance between the two centroid locations as a percentage of the wafer length. The calculation of localization error percentage, δr, can be described as

$$\delta r = \frac{|\vec{C}_L - \vec{C}_m|}{L_w} \cdot 100\%, \tag{2}$$

where $\vec{C}_L$ and $\vec{C}_m$ are the centroid locations of the cracks found, and L_w is the measured length of the wafer. Similarly, the percent error associated with the detected crack length can be written as δl described by Eq. 3

$$\delta l = \frac{|\Delta l|}{L_w} \cdot 100\%, \tag{3}$$

where Δl is the difference in scalar length of the cracks from endpoint to end point in comparison to the microscopic assessment.

Results and Discussion

Performing these calculations on 31 scanned samples of Bismuth Telluride wafers, the new scanning technique correctly identified 28 cracked wafers resulting in a 90.3% accuracy. Of the remaining wafers there was 1 false positive and 2 false negatives.

Of the 28 correctly identified wafers, the scanning technique located the centroids of each crack with a 2.2% discrepancy between centroid location detected using traditional microscope scanning. Centroid location error is calculated using Eqn. 2. Furthermore, the scanning technique yielded 17.8% error in detected crack length with respect to analyzed microscope imaging. Crack length error is calculated using Eqn. 3. The new technique was also less susceptible to incorrect characterization caused by surface defects.

The time required to obtain a full response profile of individual samples was recorded at an average 15 minutes per wafer. This time includes the initial setup of the sample and scanning equipment, point scan and resonance frequency determination, and finally the rapid resonance mode scanning at steady state excitation. This scanning time can be further reduced by implementing an automated process to determine the resonant frequencies and input them into the resonance mode scanning algorithm.

Upon further inspection of the scans yielding false negative results, both cracks are observed to exist close to the edge of the wafer (<0.25 mm) and propagate parallel to the edge. It is hypothesized that the processes applied to detect and mask the edge currently limit the accuracy of the algorithm to regions inside the bounds of the masking area.

The methods used to determine the assumed ground truth could also contribute to the 17.8% error in detected crack length. The assessment of wafer samples via composite microscopic imaging is still subject to error by surface defects and user experience. To increase confidence in the ground truth, more robust methods such as the micro-CT can be employed to verify true crack length on chosen samples.

Concluding Remarks

This paper presents a rapid non-intrusive crack detection and localization technique for thermoelectric wafers. The technique builds on recent developments of vibroacoustic excitation for crack detection using a laser Doppler vibrometer to assess vibration responses at various resonant modes. To reduce scan times at increased resolutions, this method employs a galvo mirror controlled LDV beam to perform rapid resonance mode scanning at steady state excitation frequencies. These scanning frequencies are determined by constructing an approximate mean response of each sample by inspecting the frequency response of individual points across the wafer geometry when excited by an ultrasonic chirp signal (6kHz - 40kHz). After performing rapid resonance mode scans at four resonance frequencies selected from the approximate mean response, a series of image processing techniques isolate detected cracks and quantify the location and length with respect to the wafer geometry. While this process can be further developed to increase automation in image processing and scanning frequency selection, this technique has proven to detect and locate cracks with significant accuracy while reducing reliance on more labor intensive and time consuming processes.

References

1. S. Twaha, J. Zhu, Y. Yan, and B. Li, "A comprehensive review of thermoelectric technology: Materials, applications, modelling and performance improvement," pp. 698–726, 11 2016.
2. M. A. Zoui, S. Bentouba, J. G. Stocholm, and M. Bourouis, "A review on thermoelectric generators: Progress and applications," 7 2020.
3. A. Mohan and S. Poobal, "Crack detection using image processing: A critical review and analysis," *Alexandria Engineering Journal*, vol. 57, pp. 787–798, 6 2018.
4. P. J. Schilling, B. P. R. Karedla, A. K. Tatiparthi, M. A. Verges, and P. D. Herrington, "X-ray computed microtomography of internal damage in fiber reinforced polymer matrix composites," *Composites Science and Technology*, vol. 65, pp. 2071–2078, 11 2005.
5. A. Novak, M. Bentahar, V. Tournat, R. E. Guerjouma, and L. Simon, "Nonlinear acoustic characterization of micro-damaged materials through higher harmonic resonance analysis," *NDT and E International*, vol. 45, pp. 1–8, 2012.
6. J. Greenhall, S. Grutzik, A. Graham, D. Sinha, and C. Pantea, "Nonlinear acoustic crack detection in thermoelectric wafers," *Mechanical Systems and Signal Processing*, vol. 139, p. 106598, 2020. [Online]. Available: https://www.sciencedirect.com/science/article/pii/S0888327019308192
7. A. Arena, C. Delle Piane, and J. Sarout, "A new computational approach to cracks quantification from 2d image analysis: Application to micro-cracks description in rocks," *Computers Geosciences*, vol. 66, pp. 106–120, 2014. [Online]. Available: https://www.sciencedirect.com/science/article/pii/S0098300414000107

8. T. H. Lee and K. Y. Jhang, “Experimental investigation of nonlinear acoustic effect at crack,” *NDT E International*, vol. 42, no. 8, pp. 757–764, 2009. [Online]. Available: https://www.sciencedirect.com/science/article/pii/S0963869509001169
9. I. T. Cummings, “Acoustic steady-state excitation spatial spectroscopy (assess),” Los Alamos National Laboratory (LANL), Los Alamos, NM (United States), Tech. Rep., 06 2021. [Online]. Available: https://www.osti.gov/biblio/1798098
10. J. T. Sylvain Paris, Pierre Kornprobst and F. Durand, “Bilateral filtering: Theory and applications,” *Foundations and Trends in Computer Graphics and Vision*, vol. 4, no. 1, pp. 1–10, 2009. [Online]. Available: https://www.cse.iitd.ac.in/~pkalra/col783-2017/bilateral-filtering.pdf
11. P.-Z. Tian-Shi Liu, Rui-Xiang Liu and S.-W. Pan, “Improved canny algorithm for edge detection of core image,” *Open Automation and Control Systems Journal*, vol. 7, 2014. [Online]. Available: https://benthamopen.com/contents/pdf/TOAUTOCJ/TOAUTOCJ-6-426.pdf
12. X. Zhang, Z. Tang, J. Yu, M. Guo, and L. Jiang, “Convex hull properties and algorithms,” *Applied Mathematics and Computation*, vol. 216, no. 11, pp. 3209–3218, 2010. [Online]. Available: https://www.sciencedirect.com/science/article/pii/S0096300310004728
13. P. Maragos, “Chapter 13 - morphological filtering,” in *The Essential Guide to Image Processing*, A. Bovik, Ed. Boston: Academic Press, 2009, pp. 293–321. [Online]. Available: https://www.sciencedirect.com/science/article/pii/B9780123744579000135